Journal of Hazardous Materials 194 (2011) 338–344

Contents lists available at ScienceDirect

Journal of Hazardous Materials

journal homepage: www.elsevier.com/locate/jhazmat

Alkaline hydrothermal synthesis of homogeneous titania microspheres with urchin-like nanoarchitectures for dye effluent treatments

Jin-Ming Wu [a,*], Xiao-Mei Song [a], Mi Yan [b,**]

[a] State Key Laboratory of Silicon Materials, Zhejiang University, ZheDa Road 38#, Hangzhou 310027, PR China
[b] Department of Materials Science and Engineering, Zhejiang University, ZheDa Road 38#, Hangzhou 310027, PR China

ARTICLE INFO

Article history:
Received 20 April 2011
Received in revised form 2 July 2011
Accepted 28 July 2011
Available online 10 August 2011

Keywords:
Nanostructure
Titanium oxide
Hydrothermal synthesis
Photocatalysis

ABSTRACT

The heterogeneous photocatalysis technique to treat dye effluents demands micrometer-sized titania aggregates with one-dimensional nanostructures, which possess high photocatalytic activity and at the same time facilitate the catalyst-recovery from a slurry system. In this study, the solution remained after interactions between metallic Ti and hydrogen peroxide was subjected to an alkaline hydrothermal treatment. Microspheres with extremely uniform sizes of ca. 2 μm in diameter were achieved after a subsequent proton exchange followed by calcination in air. The microspheres were urchin-like aggregates of radially assembled nanowires, which consisted of chain-like anatase single crystallites with an average diameter of 20–25 nm. The homogeneous microspheres calcinated at 600 °C possessed a surface area of 45.4 m^2/g and exhibited an excellent activity to assist photodegradation of rhodamine B in water, which is significantly higher than that of P25 titania nanoparticles. Because of the much easier recovery of the photocatalyst, the homogeneous microspheres synthesized herein may find practical applications in efficient photocatalytic treatments of dye effluents.

1. Introduction

As one of the advanced oxidation techniques for wastewater treatments, heterogeneous photocatalytic reactions utilizing titania (TiO_2) as photocatalysts are capable of decomposing organic pollutants thoroughly under a mild condition, which hence attracted much attention worldwide [1]. For photocatalysis setups, a slurry system is several times higher in efficiency when compared with an immobilized one [2]; unfortunately, the recovery of titania nanoparticles after the photocatalysis process is quite cumbersome [3]. There appeared two main approaches to alleviate the situation. One is to coat nanosized titania onto a magnetic core of iron oxides, which makes it easier to be separated from a slurry-type photoreactor under an external magnetic field [4]; however, the heterojunction formed between titania and iron oxides usually serves as additional recombination centers of photogenerated charges, which hence reduces remarkably the photocatalytic activity of titania [5]. Recently, an interlayer of silica between the magnetic core and the titania shell was reported to enhance the property of the magnetic photocatalyst [6]. In addition, Agrawal et al. [7] reported a template-assisted fabrication of hollow titania capsules containing several superparamagnetic Fe_3O_4 nanoparticles insides. Such a novel structural design avoids the heterojunction formation, which in turn achieves a photocatalytic activity comparable to that of bulk titania nanoparticles.

The other route to easier catalyst-recovery from a slurry system is to assemble titania nanoparticles to micrometer-sized spheres either utilizing templates such as silica microspheres [8] and polystyrene (PS) latexes [9], or through several template-free approaches such as sol–gel strategy [10,11], spraying hydrolysis [12], thermal hydrolysis [13–15], sonochemical reactions with the help of a triblock copolymer [16], or glycine-assisted solvothermal synthesis [17].

One-dimensional (1D) titania nanostructures of nanorods, nanotubes and nanowires, together with two-dimensional (2D) titania nanosheets, possess a photocatalytic activity superior to that of titania nanoparticles; therefore, compared with titania microspheres consisted of nanoparticles, those assembled with 1D or 2D nanostructures should be of more interesting. Micrometer-sized assembly of 1D titania nanorods (flower-like or sea-urchin-like) has been achieved by hydrothermal treatments of a mixture of $TiCl_4$, ethanol and water [18,19], a

* Corresponding author. Tel.: +86 571 87953115; fax: +86 571 87953115.
** Corresponding author. Tel.: +86 571 87952730.
E-mail addresses: msewjm@zju.edu.cn (J.-M. Wu), mse_yanmi@zju.edu.cn (M. Yan).

0304-3894/$ – see front matter © 2011 Elsevier B.V. All rights reserved.
doi:10.1016/j.jhazmat.2011.07.110

mixture of TiB_2, TiO_2 and HF [20], a mixture of TiF_4 and urea [21], or through a mild reaction of metallic Ti with H_2O_2 aqueous solution containing certain amounts of nitric acid and hexamethylenetetramine [22,23]. As examples, hydrothermal treatments of amorphous titania spheres in ammonia followed by a subsequent calcination achieved titania microspheres assembled with 2D nanosheets [24,25]. Hollow-centered titania microspheres consisted of radial arrays of nanorods [26] and {0 0 1}-facets exposed polyhedra [27] have also been reported.

Direct oxidation of metallic Ti with H_2O_2 achieved titania thin films with various structures of nanoflowers [22,23], nanorods [28,29] and nanowires [30,31]. The solution remained after the Ti–H_2O_2 reactions can serve as a precursor to deposit monolayers of single-crystalline rutile nanorods [32,33], which contributed greatly to the light response of photoelectrical thin films when embedded in nanoparticles of either anatase [34] or CdS [35]. Herein, we report the synthesis of homogeneous titania microspheres consisted of 1D anatase nanowires through an alkaline hydrothermal treatment of the remnant of Ti–H_2O_2 reactions. The achieved titania microspheres were confirmed to possess high efficiency for treatments of dye effluents.

2. Experimental

Each metallic Ti plate (99.5% in purity) with sizes of 5 cm × 5 cm × 0.01 cm was immersed in 50 ml 30 mass% H_2O_2 aqueous solution and maintained in an oven at 80 °C for 12 h. The remnant solution, which served as a titania precursor in the current investigation, contained ca. 4.3 mM Ti(IV) ions and 3.2 mass% H_2O_2 [23]. For each synthesis, 20 g NaOH was added to 50 ml precursor to give a concentration of 10 M. The addition of NaOH in the precursor resulted in the release of lots of heat, which led to a clear solution. The solution was then sealed in a Teflon-lined autoclave (60 ml in volume) and maintained at 120 °C for 20 h. After the hydrothermal reaction, the precipitates were collected by centrifugation and washed thoroughly with distilled water for three times, followed by dispersing in 0.6 M HCl aqueous solution for 12 h under ambient temperature on a shaking table to fulfill the proton exchange [26]. Finally, the precipitates were washed, collected by centrifugation, dried at 80 °C, and then subjected to heating in air for 1 h at various temperatures to allow for the titania crystallization.

The powder morphology was observed using a field emission scanning electron microscopy equipped with an energy dispersive X-ray analysis (EDS) system (FE-SEM, Hitachi S-4800, Tokyo, Japan). The high-resolution transmission electron microscope (HR-TEM) examination was employed with a JEM-2010 microscope (JEOL, Japan) working at 200 kV. The X-ray diffraction (XRD) measurements were conducted on a Rigaku D/max-3B diffractometer with CuKα radiation, operated at 40 kV, 36 mA (λ = 0.154056 nm). Nitrogen sorption measurements were conducted at 77 K using Autosorb-1-C (Quantachrome Instruments). The Brunauer–Emmett–Teller (BET) approach using desorption data and the relative pressure below 0.3 was utilized to determine the surface area. The pore size distribution and pore volume were estimated by the Barrett–Joyner–Halenda (BJH) method using the desorption curve. The sample was degassed at 150 °C to remove physisorbed gases prior to the measurement.

Aqueous rhodamine B solution with an initial concentration of 0.005 mmol/L was utilized as target molecules to evaluate the photocatalytic activity for dye-effluent treatments. The photodegradation experiments were conducted in a pyrex reactor with a water-jacket, under the illumination of a 500 W Xe-lamp (CHF-XM500, Beijing Trusttech Co. Ltd.). Before the test, 50 ml of the model solution loaded with 20 mg titania powders was subjected to ultrasonic vibration for 5 min and stirred in dark for 30 min to establish an absorption balance. During the photocatalytic reaction, the solution was stirred continuously and exposed to air. The slurry after 30 min illumination was subjected to centrifugation to separate the titania powders. The upper clear solution was then subjected to a scan from 450 to 600 nm by a UV–vis spectrophotometer (UV-1800PC, Shanghai Mapada, Shanghai, China), using a quartz cuvette of 1 cm of the optical path length. In all cases, the amount of rhodamine B absorbed on titania powders is similar to be less than 5%; therefore, for simplicity, the remained rhodamine B concentration was determined by normalizing the absorbance at the wavelength of 553 nm to that of the as-prepared 0.005 mmol/L solution.

3. Results and discussion

Fig. 1 shows the titania microspheres after the proton exchange and those followed by a subsequent calcination for 1 h at 600 and 700 °C. Homogeneous spheres with an average diameter of ca. 2 μm have been achieved after the alkaline hydrothermal treatment, which remained unchanged after the subsequent proton exchange procedure. The homogeneous microspheres were aggregations of nanowires, which remained stable after a subsequent calcination at 600 °C. The sintering of the titania nanowires was significant only after further increasing the calcination temperature to 700 °C. The proton exchange has removed thoroughly sodium ions, as confirmed by the EDS analysis (Fig. 2).

XRD patterns of the titania microspheres after the proton exchange and those followed by a subsequent calcination at various temperatures are illustrated in Fig. 3. The microspheres just after the proton exchange exhibited very weak XRD intensity with two broad peaks centered around 25° and 48° in 2θ degrees, respectively, which can be approximately contributed to monoclinic trititanic acid ($H_2Ti_3O_7$) [36,37]. After a subsequent calcination at 450 °C, the microspheres transformed remarkably to phase pure anatase, according to the standard JCPDS card No. 21-1272. With increasing calcination temperatures, the crystallinity improved, as can be discerned by the more sharp XRD peaks. The grain size was estimated to be ca. 19.4, 26.4 and 38.6 nm, for the three samples calcinated at 450, 600 and 700 °C, respectively, applying the Scherer formula [38],

$$D = \frac{0.9\lambda}{B\cos\theta} \quad (1)$$

where D is the mean particle size, λ is the wavelength of the X-ray radiation, B is the full width at half maximum (FWHM) of the characteristic peak, and θ is the diffraction angle. The anatase (0 0 4) plane located at 48.0° in 2θ was used for the calculation because of its symmetry.

The low-magnification TEM image of the microsphere subjected to a thermal treatment at 600 °C is illustrated in Fig. 4a. The microsphere as a whole exhibits a sea-urchin like morphology, which is an aggregation of titania nanowires with average diameters of ca. 20–25 nm and lengths of nearly 1 μm. A higher magnification TEM image shows that the nanowires are actually chains of anatase single-crystallites. Several single-crystalline nanorods align one by one along predominantly the axis direction of the nanowire (Fig. 4b). The upper part in Fig. 4c indicates the HR-TEM image of two neighboring nanorods labeled as A and B. Fringes with neighboring distances of 0.35 nm and 0.24 nm correspond to the interplaner distance of anatase (1 0 1)

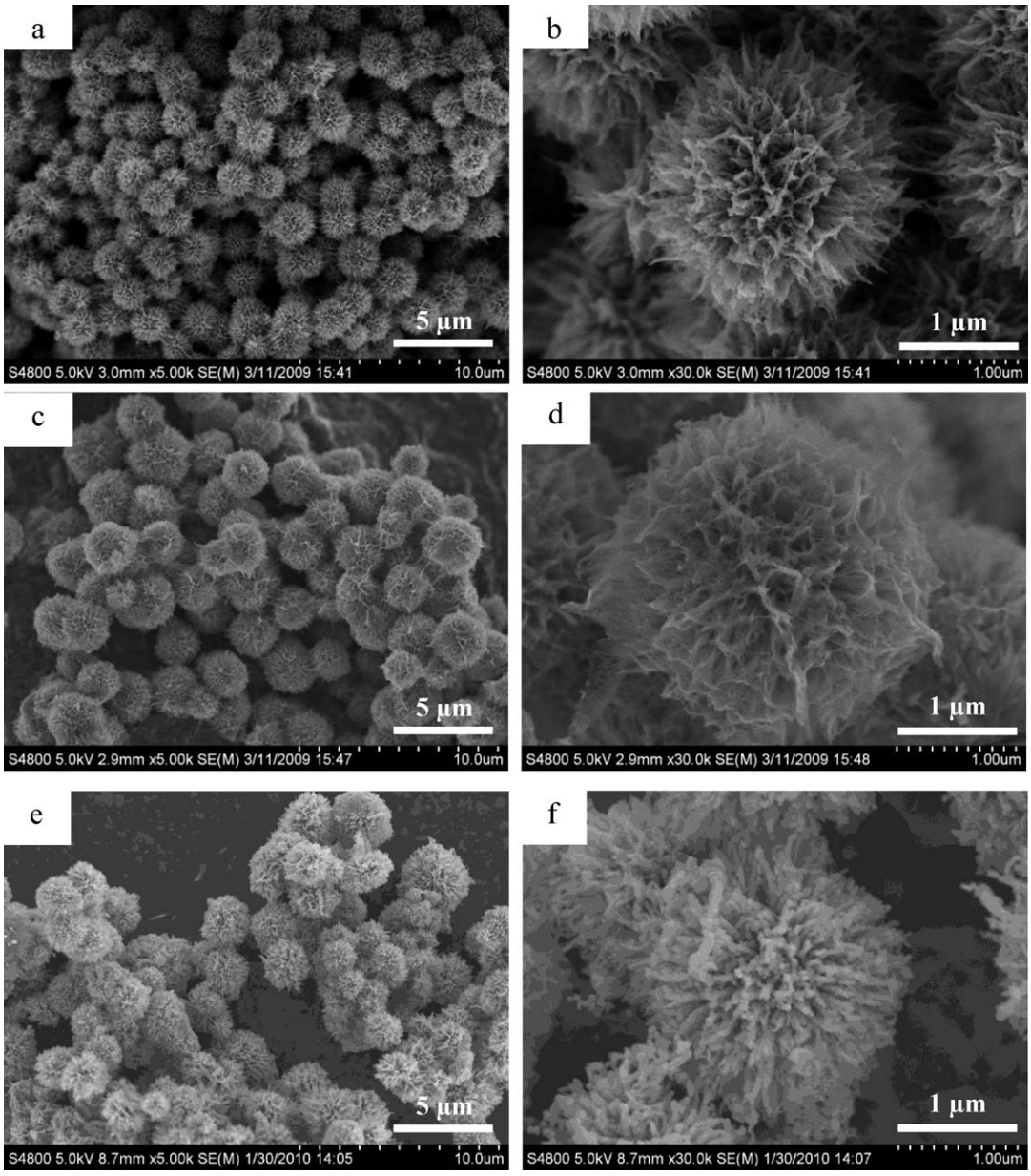

Fig. 1. FE-SEM morphologies of homogeneous titania microspheres after the proton exchange (a and b) and those followed by calcination for 1 h at 600 °C (c and d) and 700 °C (e and f).

and (0 0 4) planes, respectively. The two sets of fringes in the nanorod A aligned with an angle of ca. 68°, which is near to the theoretical value (68.3°) for the angle between the (1 0 1) and (0 0 4) facets of anatase crystals. The two parallel nanorods grew mainly along the [1 0 1] direction. The selected area electron diffraction pattern from the microsphere as a whole is typical of anatase with random grain orientations (the inset in Fig. 4c).

There appeared many reports on fabrications of titanate nanosheets, and also nanotubes and nanofibers via the subsequent folding of the nanosheets, through hydrothermal treatment of titania nanoparticles in alkaline solutions [37,39]. It is not surprising that, after a final calcination to decompose the polytitanic acid while maintaining its nanostructure, such an approach can also be applied to synthesize titania nanotubes or nanofibers [36]. Instead of titania nanoparticles, titanium aloxides such as tetrabutyl titanate [36], or the corrosion products of metallic Ti (plates or powders) with H_2O_2 [26,40], has also been utilized as precursors for the titania nanowire formation. Unlike Mao et al. [26] and Wu et al. [40], in the current investigation, the corrosive reaction between Ti and H_2O_2 has been separated from the alkaline hydrothermal treatment, which we think contributes to the formation of homogeneous titania microspheres.

Under an alkaline hydrothermal condition, the formation of titanate nanosheets proceeds in the following steps: (1) partial dissolution of the initial source of titanium (either TiO_2 or Ti) to release Ti(IV) into alkaline solution, (2) formation of titanate nanosheets with thickness of several nanometers, and (3) transformation of nanosheets to nanotubes or nanofibers [26,36,37,39]. Titanate nanosheets remain in a dynamic equilibrium with Ti(IV) in solution, the molar concentration, $c_{Ti(IV)}$, of which is dependent

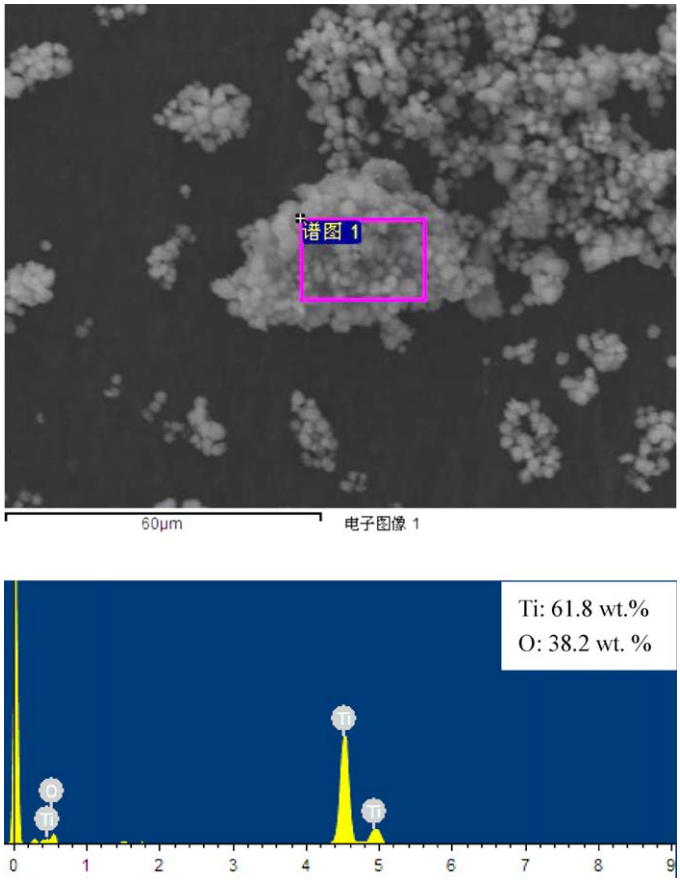

Fig. 2. EDS analysis results of titania microspheres after the proton exchange and calcinated at 600 °C for 1 h.

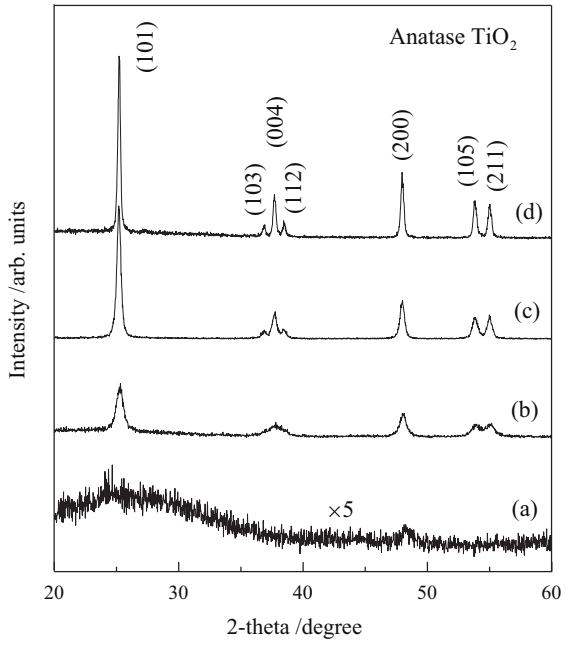

Fig. 3. XRD patterns of the titania microspheres after the proton exchange (a) and those followed by calcination for 1 h at 450 (b), 600 (c) and 700 °C (d).

on the reaction temperature T (in Celsius) through the equation follows (in 10 M NaOH) [41],

$$\ln c_{\mathrm{Ti(IV)}} = \frac{0.355 - 2623}{T + 273} \quad (2)$$

For T = 180 °C, Eq. (2) gives a value of 4.36 mM for the molar concentration of Ti(IV) ions. The precursor utilized in the current investigation contains ca. 4.3 mM Ti(IV), a value just near the equilibrium concentration of Ti(IV) in 10 M NaOH. This means a quite low supersaturation with respect to sodium titanates in the solution. Unlike the commonly adopted reactants to synthesize titanates [26,36,37,39–42], the present reactant contains no solid phase to provide sites for heterogeneous nucleation; therefore, it is expected that the sodium titanate precipitated mainly through homogeneous nucleation. The continuous growth of the nuclei is inhibited because of the relatively low supersaturation. As a result, homogeneous microspheres were achieved in the current investigation. It is noted that the hollow titanate microspheres achieved by Mao et al. [26] ranged from 0.8 to 1.2 μm in size.

A Ti(IV) concentration beyond 3.3 mM as well as intensification of the reaction through hydrothermal treatment has been argued to favor the transformation of titanate nanosheets to nanowires [37,41]. In the current investigation, the nanowires aggregated to form microspheres to minimize the surface energy of the system. The subsequent proton exchange procedure transformed sodium titanates to hydrogen titanates, maintaining the morphology unchanged. The subsequent calcination in air further decomposed hydrogen titanates to anatase, through *in situ* crystallizations. The resultant anatase nanowires consisted of single-crystalline anatase nanorods aligned along the [1 0 1] direction. The grain boundary in the nanowires is a small-angle one (Fig. 4c). It is interesting to note that a calcination temperature as high as 700 °C caused remarkable sintering of the nanowires; but the microsphere as a whole is not destroyed (Fig. 1e and f).

Fig. 5 indicates the nitrogen adsorption–desorption isotherm and the pore size distribution curve of the titania microspheres obtained by 600 °C calcination. The BET specific surface area of the microspheres is determined to be 45.4 m^2/g. The corresponding pore size distribution curve exhibits a dual pore structure of the anatase microspheres. The maxima at ca. 1.6 nm can be contributed to the defects (voids) arising from the alignment of anatase crystals within a nanowire; while the one at ca. 17.6 nm can be attributed to the intra-aggregate pore of the nanowires [42]. The microspheres possessed a mean pore size of ca. 17.7 nm and a total pore volume of 0.355 cm^3/g. The BET specific surface area achieved in the current investigation is approaching the upper limit reported for titanate nanofibers derived by reactions of titania nanoparticles with concentrated alkaline solutions, the specific surface area of which varies in the range from 20 to 50 m^2/g [37]. It is also quite impressing when compared with previously reported titania microspheres. For example, after calcinated at 500 °C, the BET specific surface area of hollow titania microspheres with mesoporous surfaces fabricated by Li et al. [12] is 38.4 m^2/g. Jitputti et al. [24] reported that titania microspheres consisted of anatase nanosheets exhibited a BET specific surface area of 31.7 m^2/g after a subsequent calcination at 500 °C for 1 h. It is noted that, the surface area of anatase powders derived by a hydrolyzing procedure reduced to 25 m^2/g upon heating at 600 °C for 2 h [43]. Coalescence of neighboring nanoparticles results in the grain growth and hence surface area reduction for condensed titania powders or films. Such a phenomenon could be alleviated to a great extent in the sea-urchin like microspheres because the titania nanowires separated from each other. It is reported that, even for low-temperature derived crystalline titania, a subsequent calcination to further improve the crystallinity of titania favors the photocatalytic activity [44]. Therefore, it is of great importance that the novel nanoarchitecture

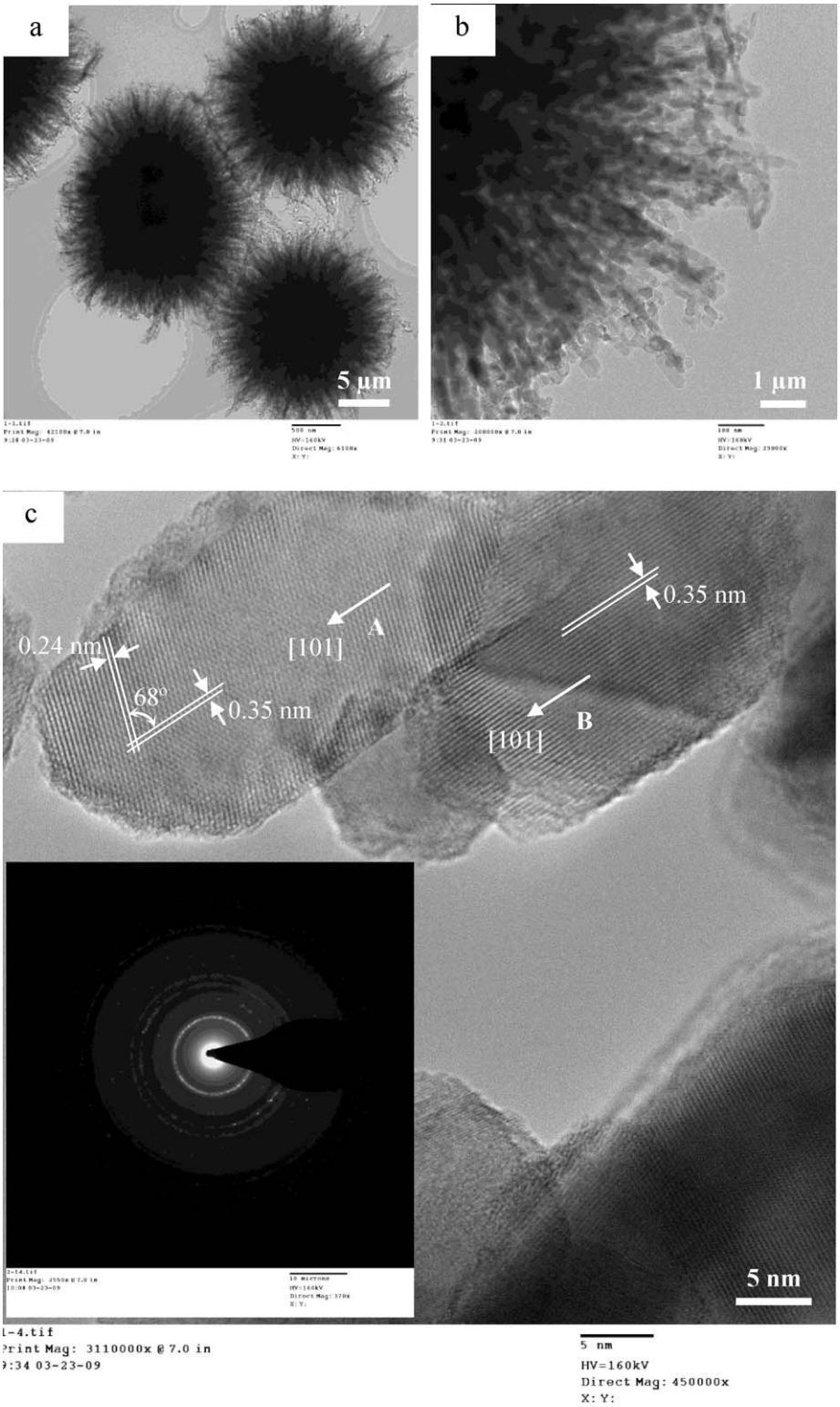

Fig. 4. Low (a) and high (b) magnification TEM images of the titania microspheres calcinated at 600 °C for 1 h. The HR-TEM image illustrating the alignment of two neighboring single-crystalline nanorods is demonstrated in (c). Inset in (c) is the selected area electron diffraction pattern collected from one microsphere.

derived in the current investigation is capable of maintaining a high specific surface area upon the subsequent thermal treatment.

Fig. 6 shows the remained concentration of rhodamine B in water after illumination for 30 min, in the presence of the titania microspheres obtained by calcination at various temperatures of 450, 600 and 700 °C. The blank test revealed that the degradation of rhodamine B under the illumination of Xe-lamp is negligible within 30 min [30]. The sample subjected to calcination at 600 °C exhibited the best activity to assist photodegradation of rhodamine B in water, which is significantly higher than that of P25, a golden

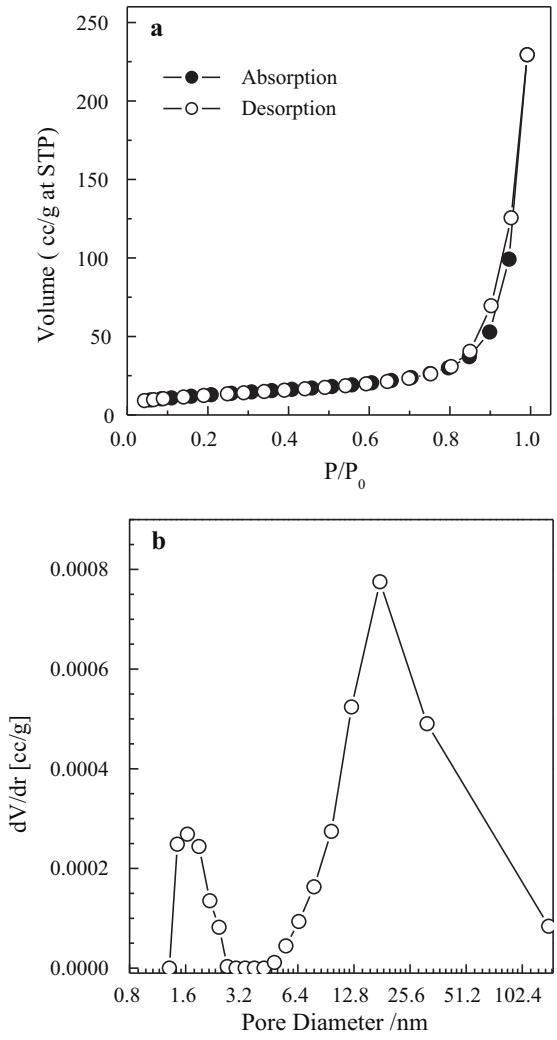

Fig. 5. Nitrogen adsorption–desorption isotherm (a) and the pore size distribution curve as determined using desorption data and the BJH model (b) for the titania microspheres calcinated at 600 °C for 1 h.

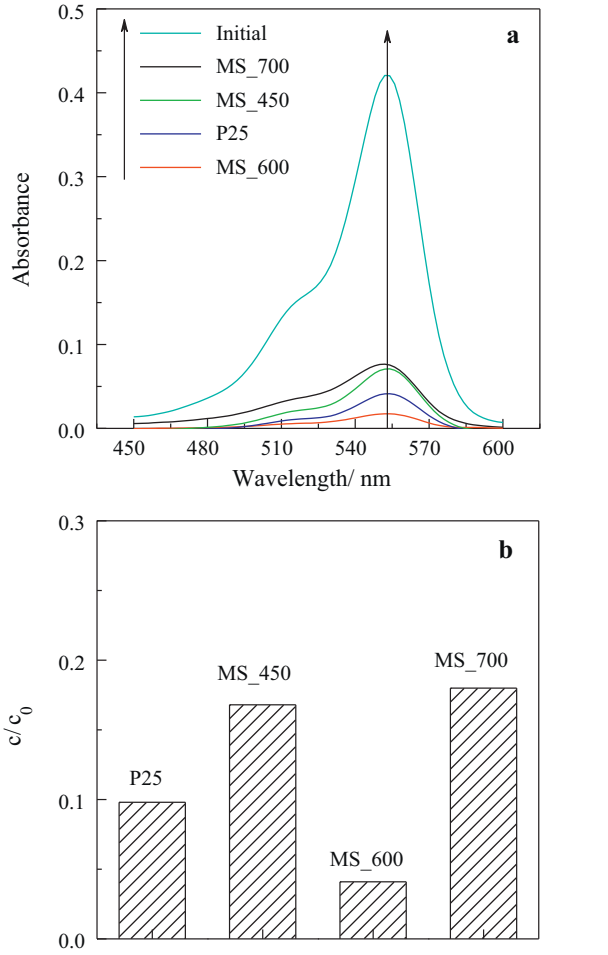

Fig. 6. (a) UV–vis absorption spectra and (b) remained normalized concentration of rhodamine B in water after illumination of 30 min, in the presence of Degussa P25 titania nanoparticles (P25) and titania microspheres (MS) after the proton exchange followed by calcination at various temperatures for 1 h.

standard photocatalyst. A lower calcination temperature resulted in insufficient crystalline; while a higher temperature led to significantly sintering of the nanowires and hence the reduced specific surface area. The high photocatalytic activity of the 600 °C calcinated microspheres can be contributed to the well balance between the crystallinity and the specific surface area. Fig. 4c illustrates that the nanowires constituting the 600 °C-calcinated microspheres are chains of 20–25 nm anatase single-crystalline nanorods. Such a novel nanostructure favors the charge separation and its migration to the surface to be involved in a photocatalytic reaction. Considering that P25 possesses an average particle size of 30 nm and a BET specific surface area of 50 m^2/g, the fact that the present titania microspheres possessed an activity to assist photodegradation of rhodamine B remarkably higher than that of P25 is of great interest in practice for treatments of dye effluents. Fig. 7a indicates that during the photodegradation reaction, the titania microspheres can be well-dispersed in water. After sedimentation for 24 h, most of the microspheres sank while P25 nanoparticles still well dispersed (Fig. 7b). This suggests that the recovery of the microspheres from the slurry will be much easier. The improved uniformity of the microspheres further facilitates the catalyst-recovery procedure.

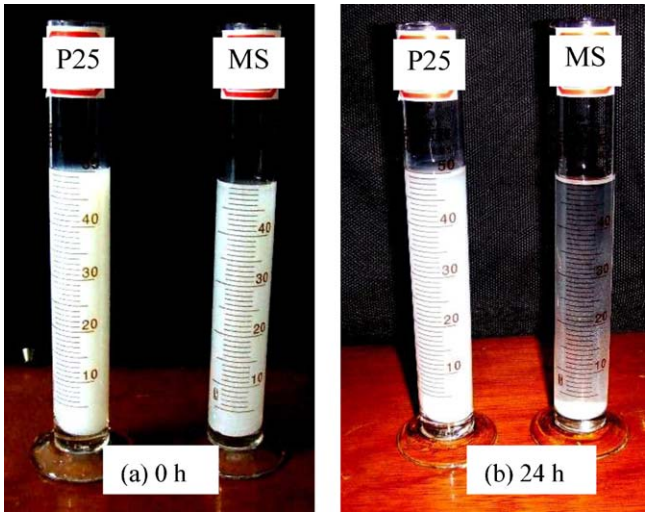

Fig. 7. Optical photos showing sedimentation of Degussa P25 titania nanoparticles (P25) and titania microspheres (MS) after the proton exchange followed by calcination at 600 °C for 1 h: (a) just after ultrasonic vibration of the slurry and (b) that after sedimentation for 24 h. The slurry was prepared by dispersing 20 mg titania particles in 50 ml distilled water.

4. Conclusions

A titania precursor containing 4.3 mM Ti(IV) ions and 3.2 mass% H_2O_2 was prepared by interactions between metallic Ti plate and 30 mass% H_2O_2 aqueous solution at 80 °C for 12 h, which was then subjected to an alkaline hydrothermal treatment at 180 °C for 20 h. After a subsequent proton exchange followed by calcination in air, homogeneous microspheres consisting of anatase nanowires were achieved. The microspheres were very uniform with sizes of 2 μm in diameter. The radially aligned nanowires consisted of chain-like single-crystalline anatase nanorods with diameters of 20–25 nm. Compared with P25 titania nanoparticles, the synthesized homogeneous anatase microspheres calcinated at 600 °C possessed a significantly higher activity to assist photodegradation of rhodamine B in water, because of the well-crystallinity and high BET specific surface area of 45.4 m^2/g.

References

[1] X. Chen, S.S. Mao, Titanium dioxide nanomaterials: synthesis, properties, modifications, and applications, Chem. Rev. 107 (2007) 2891–2959.
[2] U. Cernigoj, U.L. Stangar, P. Trebse, U.O. Krasovec, S. Gross, Evaluation of a novel carberry type photoreactor for the degradation of organic pollutants in water, J. Photochem. Photobiol. A: Chem. 188 (2007) 169–176.
[3] R.J. Braham, A.T. Harris, Review of major design and scale-up considerations for solar photocatalytic reactors, Ind. Eng. Chem. Res. 48 (2009) 8890–8895.
[4] S. Waston, D. Beydoun, R. Aml, Synthesis of a novel magnetic photocatalyst by direct deposition of nanosized TiO_2 crystals onto a magnetic core, J. Photochem. Photobiol. A: Chem. 148 (2002) 303–313.
[5] D. Beydoun, R. Amal, G.K.C. Low, S. McEvoy, Novel photocatalyst: titania-coated magnetite, activity and photodissolution, J. Phys. Chem. B 104 (2000) 4387–4396.
[6] M.M. Ye, Q. Zhang, Y.X. Hu, J.P. Ge, Z.D. Lu, L. He, Z.L. Chen, Y.D. Yin, Magnetically recoverable core-shell nanocomposites with enhanced photocatalytic activity, Chem. Eur. J. 16 (2010) 6243–6250.
[7] M. Agrawal, S. Gupta, A. Pich, N.E. Zafeiropoulos, J. Rubio-Retama, D. Jehnichen, M. Stamm, Template-assisted fabrication of magnetically responsive hollow titania capsules, Langmuir 26 (2010) 17649–17655.
[8] J.G. Yu, W. Liu, H.G. Yu, A one-pot approach to hierarchically nanoporous titania hollow microspheres with high photocatalytic activity, Cryst. Growth Des. 8 (2008) 930–934.
[9] M. Qiao, Q.A. Chen, S.S. Wu, J.A. Shen, Novel sol–gel synthesis of N-doped TiO_2 hollow spheres with high photocatalytic activity under visible light, J. Sol–Gel Sci. Technol. 55 (2010) 377–384.
[10] P.F. Lee, X.W. Zhang, D.D. Sun, J.H. Du, J.O. Leckie, Synthesis of bimodal porous structured TiO_2 microsphere with high photocatalytic activity for water treatment, Colloids Surf. A 324 (2008) 202–207.
[11] Y.C. Cheng, J.J. Guo, X.H. Liu, A.H. Sun, G.J. Xu, P. Cui, Preparation of uniform titania microspheres with good electrorheological performance and their size effect, J. Mater. Chem. 21 (2011) 5051–5056.
[12] G.H. Li, J.T. Zhu, W. Tian, C.N. Ma, Preparation and optical property of anatase hollow microsphere with mesoporosity, Mater. Res. Bull. 44 (2009) 271–275.
[13] C.H. Cho, D.K. Kim, D.H. Kim, Photocatalytic activity of monodispersed spherical TiO_2 particles with different crystallization routes, J. Am. Ceram. Soc. 86 (2003) 1138–1145.
[14] M.Z.C. Hu, V. Kurian, E.A. Payzant, C.J. Rawn, R.D. Hunt, Wet-chemical synthesis of monodispersed barium titanate particles—hydrothermal conversion of TiO_2 microspheres to nanocrystalline $BaTiO_3$, Powder Technol. 110 (2000) 2–14.
[15] X.C. Jiang, T. Herricks, Y.N. Xia, Monodispersed spherical colloids of titania: synthesis, characterization, and crystallization, Adv. Mater. 15 (2003) 1205–1209.
[16] L.Z. Zhang, J.C. Yu, A sonochemical approach to hierarchical porous titania spheres with enhanced photocatalytic activity, Chem. Commun. (2003) 2078–2079.
[17] S.J. Ding, F.Q. Huang, X.L. Mou, J.J. Wu, X.J. Lu, Mesoporous hollow TiO_2 microspheres with enhanced photoluminescence prepared by a smart amino acid template, J. Mater. Chem. 21 (2011) 4888–4892.
[18] H. Qiao, Y.W. Wang, L.F. Xiao, L.Z. Zhang, High lithium electroactivity of hierarchical porous rutile TiO_2 nanorod microspheres, Electrochem. Commun. 10 (2008) 1280–1283.
[19] Y.W. Wang, L.Z. Zhang, K.J. Deng, X.Y. Chen, Z.G. Zou, Low temperature synthesis and photocatalytic activity of rutile TiO_2 nanorod superstructures, J. Phys. Chem. C 111 (2007) 2709–2714.
[20] F. Huang, Z.Y. Fu, A.H. Yan, W.M. Wang, H. Wang, Y.C. Wang, J.Y. Zhang, Y.B. Cheng, Q.J. Zhang, Facile synthesis, growth mechanism, and UV–vis spectroscopy of novel urchin-like TiO_2/TiB_2 heterostructures, Cryst. Growth Des. 9 (2009) 4017–4022.
[21] Y. Takezawa, H. Imai, Structural control on crystal growth of titanate in aqueous system: selective production of nanostructures of layered titanate and anatase-type titania, J. Cryst. Growth 308 (2007) 117–121.
[22] J.M. Wu, B. Huang, M. Wang, A. Osaka, Titania nanoflowers with high photocatalytic activity, J. Am. Ceram. Soc. 89 (2006) 2660–2663.
[23] J.M. Wu, B. Qi, Low-temperature growth of a nitrogen-doped titania nanoflower film and its ability to assist photodegradation of rhodamine B in water, J. Phys. Chem. C 111 (2007) 666–673.
[24] J. Jitputti, T. Rattanavoravipa, S. Chuangchote, S. Pavasupree, Y. Suzuki, S. Yoshikawa, Low temperature hydrothermal synthesis of monodispersed flower-like titanate nanosheets, Catal. Commun. 10 (2009) 378–382.
[25] S. Pavasupree, S. Ngamsinlapasathian, Y. Suzuki, S. Yoshikawa, Preparation and characterization of high surface area nanosheet titania with mesoporous structure, Mater. Lett. 61 (2007) 2973–2977.
[26] Y.B. Mao, M. Kanungo, T. Hemraj-Benny, S.S. Wong, Synthesis and growth mechanism of titanate and titania one-dimensional nanostructures self-assembled into hollow micrometer-scale spherical aggregates, J. Phys. Chem. B. 110 (2006) 702–710.
[27] S.W. Liu, J.G. Yu, M. Jaroniec, Tunable photocatalytic selectivity of hollow TiO_2 microspheres composed of anatase polyhedra with exposed {0 0 1} facets, J. Am. Chem. Soc. 132 (2010) 11914–11916.
[28] J.M. Wu, Low-temperature preparation of titania nanorods through direct oxidation of titanium with hydrogen peroxide, J. Cryst. Growth 269 (2004) 347–355.
[29] J.M. Wu, Photodegradation of rhodamine B in water assisted by titania nanorod thin films subjected to various thermal treatments, Environ. Sci. Technol. 41 (2007) 1723–1728.
[30] J.M. Wu, H.X. Xue, Photocatalytic active titania nanowire arrays on Ti substrates, J. Am. Ceram. Soc. 92 (2009) 2139–2143.
[31] R.H. Tao, J.M. Wu, H.X. Xue, X.M. Song, X. Pan, X.Q. Fang, X.D. Fang, S.Y. Dai, A novel approach to titania nanowire arrays as photoanodes of back-illuminated dye-sensitized solar cells, J. Power Sources 195 (2010) 2989–2995.
[32] J.M. Wu, B. Qi, Low-temperature growth of rutile nanorod thin films and their photon-induced property, J. Am. Ceram. Soc. 91 (2008) 3961–3970.
[33] J.M. Wu, B. Qi, Low-temperature growth of monolayer rutile TiO_2 nanorod films, J. Am. Ceram. Soc. 90 (2007) 657–660.
[34] X.M. Song, J.M. Wu, M.Z. Tang, B. Qi, M. Yan, Enhanced photoelectrochemical response of a composite titania thin film with single-crystalline rutile nanorods embedded in anatase aggregates, J. Phys. Chem. C 112 (2008) 19484–19492.
[35] X.M. Song, J.M. Wu, M. Yan, Distinct visible-light response of composite films with CdS electrodeposited on TiO_2 nanorod and nanotube arrays, Electrochem. Commun. 11 (2009) 2203–2206.
[36] B. Zhao, F. Chen, H.Q. Liu, J.L. Zhang, Mesoporous TiO_2-B nanowires synthesized from tetrabutyl titanate, J. Phys. Chem. Solids 72 (2011) 201–206.
[37] D.V. Bavykin, A.N. Kulak, F.C. Walsh, Metastable nature of titanate nanotubes in an alkaline environment, Cryst. Growth Des. 10 (2010) 4421–4427.
[38] X.M. Song, J.M. Wu, G.J. Zhang, M. Yan, A dual-layer titania film with enhanced photocatalytic activity, J. Phys. Chem. C 113 (2009) 10681–10688.
[39] D.V. Bavykin, J.M. Friedrich, F.C. Walsh, Protonated titanates and TiO_2 nanostructured materials: synthesis, properties, and applications, Adv. Mater. 18 (2006) 2807–2824.
[40] Y.H. Wu, M.C. Long, W.M. Cai, S.D. Dai, C. Chen, D.Y. Wu, J. Bai, Preparation of photocatalytic anatase nanowire films by in situ oxidation of titanium plate, Nanotechnology 20 (2009) 185703.
[41] D.V. Bavykin, B.A. Cressey, M.E. Light, F.C. Walsh, An aqueous, alkaline route to titanate nanotubes under atmospheric pressure conditions, Nanotechnology 19 (2008) 275604.
[42] D.V. Bavykin, V.N. Parmon, A.A. Lapkin, F.C. Walsh, The effect of hydrothermal conditions on the mesoporous structure of TiO_2 nanotubes, J. Mater. Chem. 14 (2004) 3370–3377.
[43] B.D. Yao, Y. Zhang, H.Z. Shi, L.D. Zhang, Fractal analysis of porous polycrystalline titania by adsorption, Chem. Mater. 12 (2000) 3740–3744.
[44] J.M. Wu, B. Huang, Y.H. Zeng, Low-temperature deposition of anatase thin films on titanium substrates and their abilities to photodegrade rhodamine B in water, Thin Solid Films 497 (2006) 292–298.